HHS Public Access

Author manuscript

Int J Radiat Oncol Biol Phys. Author manuscript; available in PMC 2022 December 01.

Published in final edited form as:

Int J Radiat Oncol Biol Phys. 2021 December 01; 111(5): 1298–1309. doi:10.1016/j.ijrobp.2021.08.002.

Dosimetric uncertainties resulting from interfractional anatomic variations for patients receiving pancreas stereotactic body radiation therapy and cone-beam CT image guidance

Joshua S. Niedzielski, PhD[1,+,*], **Yufei Liu, MD**[2], **Sylvia S. W. Ng, MD, PhD**[2,#], **Rachael M. Martin, PhD**[1], **Luis A. Perles, PhD**[1], **Sam Beddar, PhD**[1], **Neal Rebueno, CMD**[1], **Eugene J. Koay, MD, PhD**[2], **Cullen Taniguchi, MD, PhD**[2], **Emma B. Holliday, MD**[2], **Prajnan Das, MD, MS**[2], **Grace L. Smith, MD, PhD**[2], **Bruce D. Minsky, MD**[2], **Ethan B. Ludmir, MD**[2], **Joseph M. Herman, MD, MSc**[2,$], **Albert Koong, MD, PhD**[2], **Gabriel O. Sawakuchi, PhD**[1,3,*]

[1]Department of Radiation Physics, The University of Texas MD Anderson Cancer Center, Houston, TX, USA

[2]Department of Radiation Oncology, The University of Texas MD Anderson Cancer Center, Houston, TX, USA

[3]The University of Texas MD Anderson Cancer Center UTHealth Graduate School of Biomedical Sciences, Houston, TX, USA

Abstract

Purpose/Objectives: To estimate the effects of interfractional anatomic changes on dose to organs-at-risk (OARs) and tumors, as measured with cone-beam computed tomography (CBCT) image guidance for pancreatic stereotactic body radiotherapy (SBRT).

Materials/Methods: We evaluated 11 patients with pancreatic cancer, whom were treated with SBRT (33–40 Gy in 5 fractions) using daily CT-on-rails (CTOR) image guidance immediately before treatment with breath-hold motion management. CBCT alignment was simulated in the treatment planning software by aligning the original planning CT to each fractional CTOR image set via fiducial markers. CTOR datasets were used to calculate fractional doses after alignment by applying the rigid shift of the planning CT and CTOR image sets to the planning treatment

[*]**Corresponding authors:** Joshua S. Niedzielski, PhD, Department of Radiation Physics, Unit 1420, The University of Texas MD Anderson Cancer Center, 1400 Pressler St, Houston, TX 77030. Tel 832-829-9942; JSNiedzielski@mdanderson.org; and Gabriel O. Sawakuchi, PhD, Department of Radiation Physics, Unit 1420, The University of Texas MD Anderson Cancer Center, 6565 MD Anderson Blvd, Houston, TX 77030-4008. Tel 713-794-4034; gsawakuchi@mdanderson.org.

[#]**Current affiliation:** Department of Radiation Oncology, University of Toronto, Toronto, ON, Canada

[$]**Current affiliation:** Department of Radiation Medicine, Northwell Health Cancer Institute, New Hyde Park, NY, USA

[+]**Author Responsible for Statistical Analyses:** Joshua S. Niedzielski, PhD, Department of Radiation Physics, Unit 1420, The University of Texas MD Anderson Cancer Center, 1400 Pressler St, Houston, TX 77030.

Author Contributions

JSN acquired, processed, and analyzed data and wrote the manuscript. JSN and GOS interpreted the data. JSN, YL and SSWN contoured the volumes. RMM, LAP, SB, NR, EJK, CT, EBH, PD, GS, BDM, EBL, JMH, and AK helped to acquire the data and provided input on the study. JSN and GOS conceptualized the project and oversaw all aspects of the work. All authors reviewed and provided feedback on the manuscript.

isocenter and recalculating the fractional dose. Accumulated dose to the gross tumor volume (GTV), tumor vessel interface (TVI), duodenum, small bowel, and stomach were calculated by summing the 5 fractional absolute dose-volume histograms (DVHs) into a single DVH for comparison with the original planned dose.

Results: Four patients had a GTV D100% of at least 1.5 Gy less than the fractional planned value in several fractions; 4 patients had fractional underestimation of duodenum dose by 1.0 Gy per fraction. The D1.0 cm^3 <35 Gy constraint was violated for at least 1 OAR in 3 patients, with either the duodenum (n=2) or small bowel (n=1) D1.0 cm^3 being higher on the accumulated dose distribution (P=0.01). D100% was significantly lower according to accumulated dose GTV (P=0.01) and TVI (P=0.02), with 4 and 2 patients having accumulated D100% ≥4 Gy lower than the planned value for the GTV and TVI, respectively.

Conclusions: For some patients, CBCT image-guidance based on fiducial alignment may cause large dosimetric uncertainties for OARs and target structures, according to accumulated dose.

INTRODUCTION

Pancreatic cancer remains challenging to treat; it is the 4th leading cause of cancer death and has a 5-year overall survival rate of less than 10%.[1] A primary reason for poor prognosis in pancreatic cancer is that surgery is the only potentially curative treatment, but less than 20% of patients present with resectable disease at diagnosis. Patients with unresectable pancreatic cancer have a 5-year survival rate of less than 5%.[2] Treatment options for unresectable pancreatic cancer are limited to either chemotherapy or chemotherapy combined with radiation therapy (RT).[3] However, combinations of chemotherapy and RT have shown mixed success in clinical trials for treating unresectable pancreatic cancer.[4–6] The limited effectiveness of RT for pancreatic cancer can be attributed to several dose-limiting effects. First, several radiosensitive organs at risk (OARs) are located next to the gross tumor volume (GTV) and tumor vessel interface (TVI), namely the duodenum, stomach, and small bowel. Second, OARs experience substantial daily variations in size and positioning due to transient interfractional motion as well as liquid and gaseous filling.[7] Finally, the small bowel, stomach, and duodenum are all extremely radiosensitive normal tissues.[8] As a result, radiation treatment planning for pancreatic cancer typically sacrifices coverage of the tumor volume, which limits the maximum achievable prescription dose.

The emergence of hypofractionated radiation therapy (HRT) and stereotactic body radiation therapy (SBRT) has allowed for highly conformal radiation dose to be delivered to the pancreas.[9] Indeed, HRT and SBRT approaches have been successful in treating pancreatic tumors,[10–12] perhaps this is due to HRT and SBRT having a higher biological effective dose than that of conventional RT.[13] Therefore, this has led to HRT and SBRT being explored as alternative treatment options in the clinical management of pancreatic cancer. Moreover, SBRT and HRT can achieve higher fractional doses than conventional RT because of steeper high-dose gradients resulting from improvements in linear accelerator design, including high-precision multi-leaf collimator technology, as well as advanced image guidance and robust motion management strategies.

Cone-beam computed tomography (CBCT) is currently the most common means of daily image guidance used for SBRT and HRT. However, CBCT does not retain the image quality of the simulation CT used for treatment planning; consequently, the radiosensitive OARs that surround the GTV are typically not discernable on daily treatment imaging. For HRT and SBRT of the pancreas, CBCT tumor visualization is often done with the aid of radiopaque fiducial markers implanted in or near the tumor to facilitate daily image guidance for aligning the target structure (i.e., GTV/TVI); however, the OARs can receive higher fractional doses than anticipated at the treatment planning stage. Moreover, the dosimetric uncertainty of OARs for patients receiving pancreas SBRT or HRT under daily CBCT image guidance has not been previously examined.

CT-on-rails (CTOR) is another in-room image guidance modality that provides diagnostic-quality CT imaging while the patient is in the treatment position immediately before or after RT.[14] CTOR can also be used to assess anatomic changes between fractions,[15] which allows CTOR imagesets to be used to quantify anatomic variations in OARs that cannot be discerned on CBCT. At our institution, patients undergoing SBRT for pancreas cancer typically receive daily RT image guidance with CTOR rather than CBCT.

The aim of this study was to assess dosimetric differences between planned and accumulated doses to the gastrointestinal luminal OARs, GTV, and TVI due to interfractional anatomic variations among patients receiving SBRT for pancreatic cancer. We used CTOR imaging immediately before each RT fraction to quantify interfractional anatomic changes and the resultant effects on dose, with the goal of estimating dosimetric uncertainties for CBCT-guided pancreas SBRT based on implanted fiducial alignment.

METHODS

Patients

This retrospective study was conducted under a protocol approved by the University of Texas-MD Anderson Cancer Center institutional review board (PA14-0646). We analyzed CT scans from 11 patients who received SBRT for pancreatic cancer in 5 fractions, with prescribed doses ranging from 33 to 40 Gy. Additional characteristics of the study patients are provided in Table E1. For all patients, daily image guidance with CTOR was used immediately before the delivery of each treatment fraction. All patients had 3–5 gold fiducial markers implanted inside or near the GTV via ultrasound-guided endoscopy by an experienced gastrointestinal surgeon before CT simulation. Patients underwent CT simulation approximately 1 week before the initiation of SBRT. Patients were immobilized in a Vac-Lok stereotactic bag (Civco Radiotherapy, Orange City, IA) and arms were positioned over the patient's head using the WingBoard system (Medtec Inc., Orange City, IA). A Philips Brilliance Big Bore CT scanner (Philips Healthcare, Andover, MA) was used to acquire simulation CT images. Planning images were acquired at 120 kVp, with a pixel size of 0.98×0.98 mm^2 and a 2.5-mm slice thickness. An infrared-based motion management system (Real-time position management system, Varian Medical Systems, Palo Alto, CA) was utilized to trace patient breathing patterns and conduct breath-hold CT imaging. For each patient, 1–3 non-contrast, followed by 3–5 contrast-enhanced, inspiration breath-hold CTs were acquired for treatment planning purposes. For contrast-enhanced CTs, a MedRad

Stellant autoinjector (Medrad Inc., Warrendale, PA) was used to intravenously deliver 150 mL of Omipaque iodinated contrast agent, (350 mg I per mL, GE Healthcare, Chicago, IL) at a flow rate of ~3–5 mL/s, to the patient during the acquisition of the 3–5 breath-hold CTs. The triphasic breath-hold CTs were acquired at approximately 30, 60, and 90 s after initiation of contrast agent injection.

The treating physician selected the optimal CT for SBRT planning. OARs were delineated on the primary contrast-enhanced CT, while the triphasic breath-hold CTs were used to delineate the GTV and TVI. Note that since various strategies were used to derive the planning target volumes (PTVs) of the 11 study patients, and to therefore maintain interpretability, the GTV and TVI were the only target structures analyzed in this study. Additional details on the delineation of the planning target volume for each of the study patients are provided in Table E2.

All patients received SBRT via step-and-shoot, intensity-modulated RT, with breath-hold used for motion management. The same motion management system utilized at simulation was used for the pre-treatment CTOR acquisition and during each fraction of radiation therapy (Real-time position management system, Varian Medical Systems). Immediately before treatment delivery, CTOR images were obtained from patients in the treatment position with a GE LightSpeed RT16 CTOR scanner (GE Healthcare, Chicago, IL). CTOR images were acquired at 120 kVp with a pixel size of 0.98×0.98 mm^2 pixel size and a 2.5-mm slice thickness. All aspects of treatment planning, as well as fiducial-based CT alignments, were conducted in RayStation version 9A (RaySearch Laboratories, Stockholm, Sweden).

Contouring and Fiducial Alignment

An overview of the data processing and analysis is shown in Figure 1. The duodenum, small bowel, stomach, TVI, and GTV were contoured on the planning CT scan and on each daily CTOR imageset by an experienced treatment planner and reviewed by a radiation oncologist, with adjustments to the contours applied when necessary. The TVI and GTV were rigidly registered from the planning to each CTOR imageset and adjusted when required. An additional planning organ-at-risk volume (PRV), derived by combining the stomach, small bowel, and duodenum contours was created to avoid ambiguity in delineating the transition regions of the gastrointestinal luminal OARs. Fiducials were delineated by segmenting the hyperintense regions on the planning CT and CTOR imagesets by using the “bone” window/level preset.

To simulate daily patient CBCT alignment before treatment, each daily CTOR image was aligned to the planning CT’s frame-of-reference by rigid registration. First, an initial manual alignment was executed to assist the automated alignment, followed by an ROI-based alignment using the fiducial contours. Every CTOR-to-planning-CT alignment was visually inspected for consistency.

Dose Accumulation and Dosimetric Analysis

After fiducial-based CT alignment, each patient’s RT plan data were loaded to each CTOR imageset for calculation of the daily accumulated dose. The treatment isocenter for each

daily fraction was determined by the corresponding shift from the originally planned isocenter, based on the fiducial alignment. A collapsed cone convolution algorithm was used to calculate the final dose, and each daily CTOR-calculated dose (referred to as "fractional dose" hereafter) was based on receiving the prescribed monitor units for a single fraction, but delivered to each respective CBCT-aligned treatment isocenter. These fractional doses were directly compared to the planned dose by calculating DVH metrics from one-fifth of the planned dose distribution.

The planned dose, fractional doses, and ROI segmentations were exported for dosimetric analysis. Dose accumulation was used to determine the final fiducial-aligned, simulated CBCT image-guided dose. The fractional absolute dose-volume histograms (DVHs) of each CTOR-based dataset were summed to create a total accumulated DVH for each OAR and target structure (hereafter referred to as "accumulated dose") by using custom-made algorithms in MATLAB (The MathWorks, Natick, MA), with which all dose accumulation calculations and dosimetric analyses were conducted. Notably, patients were not clinically treated under CBCT image guidance, and thus the accumulated doses reported here were not actually delivered but rather representations of doses these patients may have received if image guidance with CBCT had been used rather than CTOR. In addition, note that none of the study patients received daily CBCT treatment guidance; CTOR image-guidance was utilized.

Accumulated DVHs were calculated for each OAR (stomach, small bowel, duodenum, GI-PRV), the TVI and the GTV. The DVH metrics for each OAR were calculated both from the original treatment plan DVH and from the accumulated DVH, and included the following: D0.1 cm^3 (maximum dose to a 0.1 cm^3 volume within the OAR), D0.3 cm^3, D1.0 cm^3, D3.0 cm^3, and D9.0 cm^3. These DVH metrics were selected from the current clinical constraints used at our institution and from recent ASTRO guidelines.[16] The DVH metrics analyzed for the TVI and GTV included: mean dose, D100% (dose covering 100% of the GTV), D98%, D95%, and D90%.

Statistical Analysis

The paired differences in OAR, TVI, and GTV DVH metrics were analyzed by comparing the planned and accumulated doses with paired Wilcoxon signed-rank tests. Daily fractional variations in each DVH metric were also analyzed and compared. P values of <0.05 were taken to indicate statistical significance. All statistical analyses were conducted with MATLAB (The MathWorks).

RESULTS

After treatment isocenters were aligned between the planned and all fractional CTOR imagesets using implanted fiducial markers, dose and DVH metrics were calculated and accumulated on the fractional CTOR datasets. An example of interfractional anatomic variations affecting dose is shown for a patient (40-Gy prescription) in Figure 2. Notable changes in GI luminal OAR volume and position are evident. On the planning image (Fig. 2A), the duodenum (teal contour) lies outside the 28-Gy line (light blue); however, on most of the fractional CTOR images, the duodenum is included in the high-dose gradient (Fig.

2B–F; purple, orange, yellow, white colorwash). The resulting effect on dose manifests in the DVH (Fig. 2G) as much higher doses being delivered to the duodenum (solid and dashed teal lines for accumulated and planned dose, respectively), whereas coverage of the GTV decreases (solid and dashed dark blue lines for accumulated and planned dose, respectively).

Fractional variations in D1.0 cm^3, D3.0 cm^3, and D9.0 cm^3 to the duodenum, small bowel, and stomach for each patient are presented in Figure 3 and Tables E3–E5. The mean absolute fractional difference of each OAR dose metric was calculated for each patient's planned vs. accumulated dose, where the planned fractional dose was considered to be one-fifth of the planned treatment total dose and the fractional dose used for dose accumulation was calculated from each respective fraction's corresponding CTOR imageset. For most patients, large variances in fractional dose were observed for all 3 OARs (Fig. 3 and Tables 1 and E3–E5). A fractional underestimation of duodenum dose, according to planned values, by 1.0 Gy per fraction was found for 3 of the 11 patients; for some of these patients, this underestimate exceeded 1.0 Gy for several fractions (Figs. 3A–3C, Table E3).

Several patients also demonstrated notable interfractional variance in GTV and TVI coverage (Fig. 4, Tables E6–E9). Fractional GTV and TVI D100% had lower-thanplanned values of at least 2 Gy on 5 (45%) and 3 (34%) of patients, respectively. Although D95% and D90% were less sensitive (ie, more robust) to interfractional variations, 2 patients had reductions in fractional GTV coverage of at least 5 Gy for D95% and 3 Gy for D90% (Figs. 4B and 4C, Tables E6 and E7). Moreover, 4 patients had multiple fractions in which the GTV D100% was at least 1.5 Gy less than the planned value (Fig. 4A, Table E6).

The cumulative effect of fractional dosimetric variations on the OARs and GTV were reflected in the total dose differences. The total planned versus accumulated dose differences for the small bowel, stomach, duodenum, and GI-PRV D1.0 cm^3 are illustrated in Figure 5A–D. For many patients, large differences in accumulated vs. planned D1.0 cm^3 were observed for all 3 of these OARs and for all other DVH metrics as well (Table 1). Compared with planned dose, 9 patients showed larger accumulated total dose for at least 1 OAR. Moreover, the D1.0 cm^3 <35 Gy constraint was violated for 4 of the 11 study patients for at least 1 of the duodenum, stomach, or small bowel according to accumulated dose values; notably, no violations were noted on those patients' planned dose distributions. In addition, as the volume of the constraint increased (i.e., from D1.0 cm^3 to D9.0 cm^3), the extent of the increase in accumulated dose over planned dose decreased. Relative to the planned dose, all dose metrics for the GI-PRV were significantly higher for the accumulated dose distribution (Table 1).

Several patients had notable reductions in TVI and GTV total dose coverage. Comparisons of planned and accumulated dose for GTV and TVI D100% are shown in Figures 5E and 5F and Tables E6 and E7. The accumulated GTV D100% was lower than the planned value for 8 of the 11 study patients; this difference exceeded 5 Gy for 4 patients. Although D95% was more robust to interfractional variations (Fig. 4B, Table E6), 2 patients still had at least a 5-Gy loss of total, a trend also observed for all other GTV dose metrics analyzed (Tables 1, E6, and E7). A similar trend was discovered for the TVI, as D95% was more robust to interfractional variations (Fig. 4E, Table E8), yet 1 patient still had a 3-Gy loss of total TVI

coverage. Similar results were discovered for all other TVI dose metrics analyzed (Tables 1, E8, and E9).

DISCUSSION

In this study, we simulated CBCT-guided fractional SBRT doses by using daily CTOR imagesets with rigid image alignment according to implanted fiducial markers, accumulated the fractional doses, and then compared the results with the dose of the original treatment plan. These dosimetric uncertainties, which resulted from interfractional changes in patient anatomy, were determined for OARs that may not be readily discernible on CBCT, which is the standard image-guidance technique for HRT and SBRT of pancreatic cancer. We found that many patients not only received higher dose to the OARs but also experienced large reductions in both the GTV and TVI dose (relative to the original planning dose distribution). Moreover, large variations in fractional doses were found for all OARs, the TVI, and the GTV. To our knowledge, this is the first dosimetric study to analyze variations in the fractional, in addition to total, radiation dose of patients receiving SBRT for pancreatic cancer using simulated CBCT image guidance.

Many of the patients in our study had a large range of interfractional variations in OAR and GTV dose. For example, 1 patient had an average fractional accumulated D1.0 cm^3 of the duodenum that was 2.5 Gy higher than planned fractional dose; in fact, every fraction had a duodenal D1.0 cm^3 that was at least 2.0 Gy greater than the planned value. By contrast, another patient had a single fraction with a 1.1 Gy higher accumulated duodenum D1.0 cm^3, but the other 4 fractions had approximately half the fractional dose increase to the accumulated duodenum DVH. These findings illustrate the considerable heterogeneity in the OAR dose differences between planned and accumulated dose distributions among our study population.

Consistent interfractional dose differences resulted in significantly higher OAR dose when comparing planned dose distribution with accumulated dose distributions. This finding emphasizes the clinical reality that interfractional changes in OAR anatomy, especially the mobile GI luminal structures whose shape and location can change markedly secondary to gas and peristalsis, can lead to violations of normal tissue constraints. Moreover, for 3 of our 11 study patients that had plans deemed acceptable, with no violations of OAR constraints, did in fact have violation of the D1.0 cm^3 <35 Gy planning goal, according to the accumulated dose. Although beyond the scope of this study, future work should examine how these dose differences may be related to the incidence and severity of normal tissue toxicity from pancreatic SBRT.

The duodenum consistently received the highest dose of any of the 3 OARs examined in this work. This result is not surprising as most patients had gross disease of the pancreatic head. In contrast, the D1.0 cm^3 <35 Gy constraint for the stomach was never violated in either planned or accumulated dose. Several patients did have larger accumulated small bowel D1.0 cm^3 than planned, with the D1.0 cm^3 <35 Gy constraint being violated for 1 patient.

For all 3 OARs, the magnitude of dose differences between planned and accumulated dose declined as larger absolute volumes of normal tissue dose were examined (e.g., from D0.1 cm^3 to D9.0 cm^3). This result, along with examination of each individual's SBRT plans, shows that these dose differences are relegated to relatively small volumes near the GTV. This in turn demonstrates the importance of robust, daily image guidance, not just for target volume alignment but also for visualization of nearby OARs to prevent radiation-induced toxicity. For many of the patients in this small study, CBCT image guidance was adequate to preserve minimal OAR dose; however, this was not the case for several patients. This finding is consistent with those of another recent study examining interfractional anatomic variations in 35 patients treated with Cyberknife for unresectable pancreatic cancer.[17] That study showed that 83% of patients had higher accumulated than planned OAR maximum dose of <35 Gy. The same group developed an OAR motion model that could predict if plans for a given patient would be at risk for violating OAR constraints.[18] Future strategies such as this could be implemented at the treatment planning stage to identify patients at high risk of excessive OAR dose, with preemptive action taken to prevent normal tissue toxicity.

Notably, all patients in the current study underwent treatment simulation and treatment while using inspiration breath-hold for motion management, with no abdominal compression. Other motion management techniques routinely applied in pancreatic SBRT and HRT include 4DCT with or without active breathing control, dynamic gating, and abdominal compression.[19,20] One group found that respiratory gating was significantly better at intrafractional motion mitigation than abdominal compression for pancreatic cancer patients receiving SBRT.[21] An interesting comparison would be between our results and those of patients receiving pancreas SBRT or HRT for whom other motion management strategies were used.

Recently, adaptive pancreas radiation therapy under MR image-guidance has been investigated. Bohoudi et al. developed a rapid daily online adaptive SBRT planning strategy using an artificial neural network to develop daily plans on a 0.35 T MR-linac system with a 40-Gy prescription delivered in 5 fractions.[22] They found that OAR recontouring was only necessary at a distance of 3 cm from the PTV and thus demonstrated that this rapid approach was clinically feasible. Furthermore, the study by Bohoudi et al. was also consistent with our results that interfractional changes in the GI luminal OARs were random in nature. Similar to the above study, Henke et al. prescribed 50 Gy in 5 fractions in a phase I clinical trial for oligometastatic and unresectable cancers of the abdomen[23,24] and demonstrated that daily online adaptive SBRT with dose escalation was feasible in the abdomen, provided that there is high quality image guidance. Furthermore, Henke et al. found that OAR constraints for the GI luminal structures would have been violated without daily adaptation, according to delivered dose, in 22, 14, and 37 fractions for the stomach, duodenum, and small bowel, respectively, out of a total 47 treatment fractions for the study population.[24] Magallon-Baro et al. showed that adaptive SBRT using CTOR image guidance was feasible and enable to optimize PTV and GTV coverage[25]; their findings are consistent with our study in that without adaptation, 21 out of 70 total fractions examined from the entire cohort had a median D1.0 cm^3 value greater than 35 Gy for the duodenum (after scaling each fraction to a full treatment course).

Our work had several limitations. First, although interfractional motion has a primary role in dosimetric uncertainties, intrafractional motion also contributes to this effect. One group found that real-time, fiducial-based pancreatic tumor tracking could improve target coverage in ~32% of patients receiving SBRT.[26] They further found that after an initial CBCT-based alignment, a median re-alignment shift of 5.2 mm was necessary to regain target coverage. In another study involving fiducial-based tumor tracking of the pancreatic tumors under breath-hold, the mean extent of organ motion was found to be 4.2 mm and 2.7 mm in the superior-inferior and anterior-posterior directions, resepctively.[27] Collectively, these results suggest that intrafractional motion of tumor, and potentially OARs, may also influence dose uncertainties, but the magnitude of this effect remains unclear.

Another limitation of this study is that we used DVH accumulation to calculate accumulated dose and to determine dosimetric differences. Ideally, voxel-based dose could identify small regions of dose change, which is particularly relevant for the GI luminal OARs. However, deformable registration, which would be necessary for such a voxel-based analysis, is extremely challenging for the GI luminal OARs.[28] For example, Ziegler et al. examined interfractional changes to abdominal anatomy and the impact on accumulated dose using planning CTs deformed to daily treatment CBCT images using DIR.[29] They found that the duodenum and stomach had accumulated vs. planning dose differences for V39 of up to ±2.0 cm for some patients. Regarding uncertainties with DIR, the authors point to anatomical changes in the GI luminal OARs as a primary cause, which resulted in large residual errors, although specific values were not provided. Moreover, Wang et al. evaluated several deeplearning auto-segmentation algorithms for the abdominal anatomy and found that the luminal GI OARs had the poorest results, with median Dice-Sorensen similarity coefficients of 70% for the duodenum and small bowel.[30]

The aforementioned issues with DIR of the luminal OARs are the primary reasons why DVH accumulation was utilized in our study; however, DVH accumulation also has limitations. For example, Andersen et al. examined differences between dose accumulation of the bladder by DVH summation and DIR for 47 patients treated for cervical cancer and found dose deviations for D0.1cm^3 and D2.0cm^3 of greater than 5% occurring in 38% and 2% of patients, respectively.[31] This study is illustrative of the “worst case assumption” mentioned in the GEC-ESTRO II report by Potter et al. and the result of tumor shrinkage.[32] However, Gelover et al. found that DVH summation actually underestimated, not overestimated, the delivered OAR dose by 8% and 5%, for D0.1cm^3 and D2.0cm^3, respectively.[33] In addition, the GEC-ESTRO report[32] highlights the potential error in maximum doses to subvolumes of an OAR if the regions are non-contiguous; in other words if the D2.0cm^3 subvolume is located in disconnected regions of the OAR in question, then there exists substantial error in the analysis. This scenario is highly relevant for the GI luminal OARs, where maximum subvolume doses are of primary concern and non-contiguous regions of the OARs can exist near the target volume. For our study, D1.0cm^3 was the primary OAR dose of interest and was found to be less variable than smaller subvolume maximum doses. Moreover, all dose distributions on each patient where visually inspected to ensure all analyzed OAR subvolume dose distributions were contiguous.

The final limitation of our study was that we used contours on the CTOR imagesets, which do not have contrast enhancement, thereby introducing some uncertainty associated with contouring. However, in our secondary analysis of the effect of contouring variability (Supplementary Materials), we examined changes in GTV D100% and OAR D1.0 cm^3 for the 4 patients for whom the 35 Gy constraint was violated according to accumulated dose. By expanding and contracting the respective ROIs by 1 mm and 2 mm on the CTOR datasets and examining the change in dose, we showed that the OAR D1.0 cm^3 was robust to minor variability in contouring (Suppl. Fig. E1). In addition, we also examined the possible effects of contouring variations on GTV coverage (Supplementary Materials). The difference in GTV size between the total accumulated GTV and the planned GTV was compared to differences in planned vs. accumulated D100%. For the 3 patients with >20% reductions in of GTV D100%, according to accumulated dose, no trend with GTV size difference was found (Suppl. Fig. E2, Suppl. Table E10). In addition, the standard deviation of fractional GTV size was compared to the differences in planned vs. accumulated D100%. No relationship between dose differences and higher variance in fractional GTV size was found (Suppl. Fig. E3, Suppl. Table E10).

While this work simulated simple CBCT image-guidance, there are several strategies can be implemented to increase the robustness of this technique. First, the use of oral contrast may allow for improved visualization of the GI luminal OARs.[34] Another method is the use of breath-hold CBCT[35] and 4D CBCT[36]. In some patients these modalities may be able to reveal the GI luminal anatomy, and thus aid in preventing violation of OAR constraints. Related to this would be use of isodose lines from the planning dose distribution, which could be imported to the CBCT as regions of interest for alignment purposes. However, it is not clear how accurate a representation of the daily delivered dose these isodose lines might be; future studies should examine the accuracy of this technique. Taken together, the aforementioned strategies, particularly when combined, may allow for robust pancreatic radiation therapy. Future studies should compare these CBCT-based strategies to more advanced techniques, such as CTOR or MRI image-guidance.

The findings of our work open several avenues for future study. First, the large variance in interfractional doses, as well as the large differences in planned and accumulated dose, motivates daily CTOR-guided or MRI-guided adaptive SBRT and HRT for pancreatic cancer. Similar work has been accomplished for prostate cancer.[14,15] One group has already demonstrated the feasibility of adaptive re-planning for pancreatic SBRT, with improved GTV coverage and lower OAR doses.[37] Our results also support further study of selective dose-escalation for particular patients undergoing SBRT or HRT; another group found that dose-escalated SBRT of up to 60 Gy was feasible.[38] Considerations of daily anatomic variations may also enable further dose escalation in at least some patients. For example, one group showed that manual shifts of the daily treatment isocenter by using CTOR image guidance could reduce liver PTV margins by up to 5 mm.[39] Moreover, the effects of interfractional anatomic variations, and the resulting dose differences, on normal tissue toxicity should be examined. Such a study could affect OAR dose constraints as more information on delivered dose, and subsequent toxicity, is collected and analyzed. Finally, the results of this work suggest that CBCT image-guidance should be rigorously evaluated for each pancreatic SBRT treatment. Strategies could include oral contrast for

OAR localization, optimized CBCT acquisition protocols, and isodose line visualization overlayed on the CBCT from the planning CT. In addition, as advanced CBCT image-guidance modalities with improved image quality become available, identification of OARs and target structures may become more feasible.

Conclusions

Many pancreatic cancer patients under CBCT image guidance experience interfractional variations in anatomic structures, which may result in differences between planned and accumulated DVH metrics that lead to violation of OAR dose constraints. CBCT image guidance alone may not provide adequate information to avoid gastrointestinal luminal OARs. Finally, the extent of the interfractional dosimetric variance in OARs and in the GTV found here warrants further study of daily adaptive treatment approaches for pancreas RT, specifically those utilizing daily CBCT image guidance.

Supplementary Material

Refer to Web version on PubMed Central for supplementary material.

Acknowledgments

The authors thank and Christine F. Wogan, MS, ELS, of the Division of Radiation Oncology at MD Anderson for editorial contributions to early versions of this manuscript.

Funding:

Supported in part by Cancer Center Support (Core) Grant P30 CA016672 from the National Cancer Institute, National Institutes of Health, to The University of Texas MD Anderson Cancer Center.

Conflict of Interest Statement for All Authors:

GOS has a research contract with Alpha Tau Medical. PD reports honorarium from Adlai Nortye, ASTRO, and NCI/Leidos. EBH reports support from Merck. EJK reports grants from Philips Healthcare, Elekta, NIH, Stand up to Cancer, and GE, as well as personal fees from Taylor and Francis, and RenovoRx. AK reports stock in Aravive, Inc. GLS reports grants from the NCI, MD Anderson Cancer Center, and the Andrew Sabin Family Foundation. CT reports consulting fees from Xerient, and Accuray. All authors declare no conflicts of interest with the work reported here.

Data Availability Statement for the Work:

Research data are stored in an institutional repository and will be shared upon request to the corresponding author.

REFERENCES

1. Siegel RL, Miller KD, Jemal A. Cancer statistics, 2020. CA Cancer J Clin 2020;70(1):7–30. doi:10.3322/caac.21590 [PubMed: 31912902]
2. Balaban EP, Mangu PB, Yee NS. Locally advanced unresectable pancreatic cancer: American Society of Clinical Oncology Clinical Practice Guideline Summary. J Oncol Pract 2017;13(4):265–269. [PubMed: 28399382]
3. Wolfgang CL, Herman JM, Laheru DA, et al. Recent progress in pancreatic cancer. CA Cancer J Clin 2013;63(5):318–348. [PubMed: 23856911]

4. Hammel P, Huguet F, van Laethem J-L, et al. Effect of chemoradiotherapy vs chemotherapy on survival in patients with locally advanced pancreatic cancer controlled after 4 months of gemcitabine with or without erlotinib: The LAP07 randomized clinical trial. JAMA 2016;315(17):1844–1853. [PubMed: 27139057]
5. Chauffert B, Mornex F, Bonnetain F, et al. Phase III trial comparing intensive induction chemoradiotherapy (60 Gy, infusional 5-FU and intermittent cisplatin) followed by maintenance gemcitabine with gemcitabine alone for locally advanced unresectable pancreatic cancer. Definitive results of the 2000–01 FFCD/SFRO study. Ann Oncol 2008;19(9):1592–1599. [PubMed: 18467316]
6. Loehrer PJ, Feng Y, Cardenes H, et al. Gemcitabine alone versus gemcitabine plus radiotherapy in patients with locally advanced pancreatic cancer: An Eastern Cooperative Oncology Group trial. J Clin Oncol 2011;29(31):4105–4112. [PubMed: 21969502]
7. Loi M, Magallon-Baro A, Suker M, et al. Pancreatic cancer treated with SBRT: Effect of anatomical interfrac-tion variations on dose to organs at risk. Radiother Oncol 2019;134:67–73. doi:10.1016/j.radonc.2019.01.020. [PubMed: 31005226]
8. de Geus SWL, Eskander MF, Kasumova GG, et al. Stereotactic body radiotherapy for unresected pancreatic cancer: A nationwide review. Cancer 2017;123(21):4158–4167. doi:10.1002/cncr.30856. [PubMed: 28708929]
9. Ng SP, Herman JM. Stereotactic radiotherapy and particle therapy for pancreatic cancer. Cancers 2018;10(3):75.
10. Krishnan S, Chadha AS, Suh Y, et al. Focal radiation therapy dose escalation improves overall survival in locally advanced pancreatic cancer patients receiving induction chemotherapy and consolidative chemoradiation. Int J Radiat Oncol Biol Phys 2016;94(4):755–765. [PubMed: 26972648]
11. Koong AC, Le QT, Ho A, Fong B, Fisher G, Cho C, et al. Phase I study of stereotactic radiosurgery in patients with locally advanced pancreatic cancer. Int J Radiat Oncol Biol Phys 2004;58(4):1017–21. [PubMed: 15001240]
12. Herman JM, Chang DT, Goodman KA, et al. Phase 2 multi-institutional trial evaluating gemcitabine and stereotactic body radiotherapy for patients with locally advanced unresectable pancreatic adenocarcinoma. Cancer 2015;121(7):1128–1137. doi:10.1002/cncr.29161. [PubMed: 25538019]
13. Brown JM, Carlson DJ, Brenner DJ. The tumor radiobiology of SRS and SBRT: are more than 5 Rs involved? Int J Radiat Oncol Biol Phys 2014;88(2):254–262. doi:10.1016/j.ijrobp.2013.07.022 [PubMed: 24411596]
14. Liu F, Ahunbay E, Lawton C, Li XA. Assessment and management of interfractional variations in daily diagnostic-quality-CT guided prostate-bed irradiation after prostatectomy. Med Phys 2014;41(3):031710. doi:10.1118/1.4866222. [PubMed: 24593714]
15. Li X, Quan EM, Li Y, et al. A fully automated method for CT-on-rails-guided online adaptive planning for prostate cancer intensity modulated radiation therapy. Int J Radiat Oncol Biol Phys 2013;86(5):835–841. doi:10.1016/j.ijrobp.2013.04.014. [PubMed: 23726001]
16. Palta M, Godfrey D, Goodman KA, et al. Radiation therapy for pancreatic cancer: Executive Summary of an ASTRO Clinical Practice Guideline. Pract Rad Oncol 2019;9:322–332.
17. Loi M, Magallon-Baro A, Suker M, van Eijck C, Sharma A, Hoogeman M, Nuyttens J. Pancreatic cancer treated with SBRT: Effect of anatomical interfraction variations on dose to organs at risk. Radiother Oncol 2019;134:67–73. [PubMed: 31005226]
18. Magallon-Baro A, Loi M, Milder MTW, Granton PV, Zolnay AG, Nuyttens JJ, Hoogeman MS. Modeling daily changes in organ-at-risk anatomy in a cohort of pancreatic cancer patients. Radiother Oncol 2019;134:127–134. [PubMed: 31005206]
19. Keall PJ, Mageras GS, Balter JM, Emery RS, Forster KM, Jiang SB, et al. The management of respiratory motion in radiation oncology report of AAPM Task Group 76. Med Phys 2006;33(10):3874–900. [PubMed: 17089851]
20. Dieterich S, Green O, Booth J. SBRT targets that move with respiration. Physica Medica 2018;56(June 2017):19–24. [PubMed: 30527085]

21. Campbell WG, Jones BL, Schefter T, Goodman KA, Miften M. An evaluation of motion mitigation techniques for pancreatic SBRT. Radiother Oncol 2017;124(1):168–173. [PubMed: 28571887]
22. Bohoudi O, Bruynzeel AME, Senan S, Cuijpers JP, Slotman BJ, Lagerwaard FJ, Palacios MA. Fast and robust online adaptive planning in stereotactic MR-guided adaptive radiation therapy (SMART) for pancreatic cancer. Radiother Oncol 2017;125(3):439–444. [PubMed: 28811038]
23. Henke L, Kashani R, Yang D, Zhao T, Green O, Olsen L, et al. Simulated online adaptive magnetic resonance-guided stereotactic body radiation therapy for the treatment of oligometastatic disease of the abdomen and central thorax: Characterization of potential advantages. Int J Radiat Oncol Biol Phys 2016;96(5):1078–1086. [PubMed: 27742541]
24. Henke L, Kashani R, Robinson C, Curcuru A, DeWees T, Bradley J, et al. Phase I trial of stereotactic MR-guided online adaptive radiation therapy (SMART) for the treatment of oligometastatic or unresectable primary malignancies of the abdomen. Radiother Oncol 2018;126(3):519–526. [PubMed: 29277446]
25. Magallon-Baro A, Milder MTW, Granton PV, Nuyttens JJ, Hoogeman MS. Comparison of daily online plan adaptation strategies for a cohort of pancreatic cancer patients treated with SBRT. Int J Radiat Oncol Biol Phys 2021:S0360–3016(21)00312–6.
26. Vinogradskiy Y, Goodman KA, Schefter T, Miften M, Jones BL. The clinical and dosimetric impact of real-time target tracking in pancreatic SBRT. Int J Radiat Oncol Biol Phys 2019;103(1):268–275. [PubMed: 30145394]
27. Lens E, van der Horst A, Versteijne E, Bel A, van Tienhoven G. Considerable pancreatic tumor motion during breath-holding. Acta Oncol 2016;55(11):1360–1368. [PubMed: 27583771]
28. Liu Y, Lei Y, Wang T, Fu Y, Tang X, Curran WJ, et al. CBCT-based synthetic CT generation using deep-attention cycleGAN for pancreatic adaptive radiotherapy. Med Phys 2020;47:2472–2483. [PubMed: 32141618]
29. Ziegler M, Nakamura M, Hirashima H, Ashida R, Yoshimura M, Bert C, et al. Accumulation of the delivered treatment dose in volumetric modulated arc therapy with breath-hold for pancreatic cancer patients based on daily cone beam computed tomography images with limited field-of-view. Med Phys 2019;46:2969–2977. [PubMed: 31055859]
30. Wang Y, Zhou Y, Shen W, Park S, Fishman EK, Yuille AL. Abdominal multi-organ segmentation with organ-attention networks and statistical fusion. Med Image Anal 2019;55:88–102. [PubMed: 31035060]
31. Andersen ES, Noe KØ, Sørensen TS, Nielsen SK, Fokdal L, Paludan M, et al. Simple DVH parameter addition as compared to deformable registration for bladder dose accumulation in cervix cancer brachytherapy. Radiother Oncol 2013;107(1):52–57. [PubMed: 23490266]
32. Pötter R, Haie-Meder C, Van Limbergen E, Barillot I, De Brabandere M, Dimopoulos J, et al. Recommendations from gynaecological (GYN) GEC ESTRO working group (II): concepts and terms in 3D image-based treatment planning in cervix cancer brachytherapy-3D dose volume parameters and aspects of 3D image-based anatomy, radiation physics, radiobiology. Radiother Oncol 2006;78(1):67–77. [PubMed: 16403584]
33. Gelover E, Katherine C, Mart C, Sun W, Kim Y. Patient's specific integration of OAR doses (D2 cc) from EBRT and 3D image-guided brachytherapy for cervical cancer. J Appl Clin Med Phys 2018;19(2):93–92. [PubMed: 29322625]
34. Chu KY, Eccles CL, Baker T, Durrant L, Holyoake D, Robinson M, et al. Oral contrast improves soft tissue matching in image guided radiation therapy for gastrointestinal (GI) tumors. Int J Rad Biol Phys 2016;96(2):E170–E171.
35. Nakamura M, Akimoto M, Ono T, Nakamura A, Kishi T, Yano S, et al. Positional variation in pancreatic tumors using daily breath-hold cone-beam computed tomography with visual feedback. J Appl Clin Med Phys 2015;16(2):108–116.
36. Sonke JJ, Zijp L, Remeijer P, van Herk M. Respiratory correlated cone beam CT. Med Phys 2005;32(4):1176–1186. [PubMed: 15895601]
37. Li Y, Hoisak JDP, Li N, Jiang C, Tian Z, Gautier Q, et al. Dosimetric benefit of adaptive re-planning in pancreatic cancer stereotactic body radiotherapy. Med Dosim 2015;40(4):318–324. [PubMed: 26002122]

38. Colbert LE, Rebueno N, Moningi S, Beddar S, Sawakuchi GO, Herman JM, et al. Dose escalation for locally advanced pancreatic cancer: How high can we go? Adv Radiat Oncol 2018;3(4):693–700. 10.1016/j.adro.2018.07.008 [PubMed: 30370371]

39. Choi GW, Suh Y, Das P, Herman J, Holliday E, Koay EJ, et al. Assessment of setup uncertainty in hypofractionated liver radiation therapy with a breath-hold technique using automatic image registration–based image guidance. Radiat Oncol 2019;14:154. 10.1186/s13014-019-1361-6. [PubMed: 31470860]

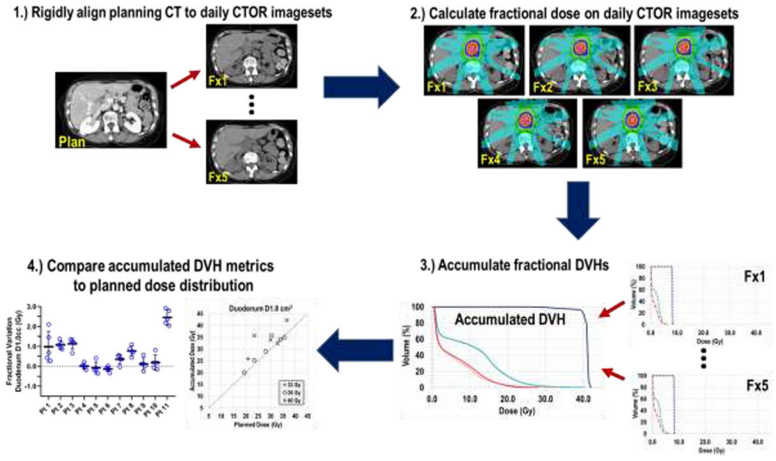

Fig. 1.

Overview of study workflow. Planning and each CTOR imageset were rigidly aligned to implanted fiducials to mimic CBCT alignment. Next, fractional doses were determined by loading the original plan information to each CTOR and delivering the treatment based on the fiducial alignment. From the absolute fractional DVHs, dose to the TVI, GTV, and OARs were accumulated by DVH summation. Finally, fractional and total dose variations were analyzed.

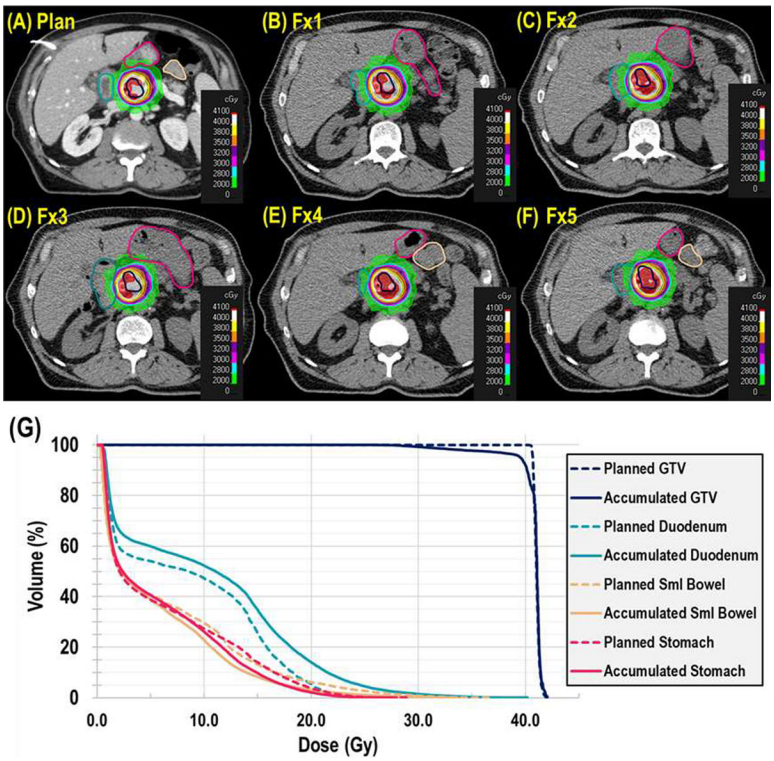

Fig. 2.

Anatomic variations affecting the dose distribution in a representative patient, with comparison of planned dose (A) to each fractional (Fx) dose (B–F). Each axial CT image is shown at the respective treatment isocenter, with the duodenum (teal), small bowel (beige), stomach (red) and gross tumor volume (GTV; dark blue) contours displayed with colorwashes of the treatment dose. (G) Dose-volume histogram comparison of the planned dose distributions (dashed lines) and the accumulated dose distributions (solid lines) for the duodenum (teal), small bowel (beige), stomach (red) and GTV (dark blue).

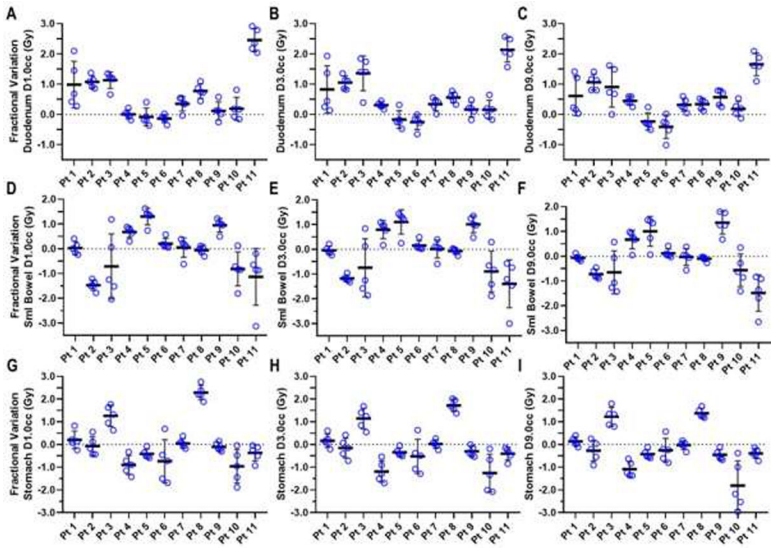

Fig. 3.

Variations in interfractional dose, measured as the absolute dose difference between the plan metric value and that of each fractional accumulated value, for duodenum (A–C), small bowel (D–F), and stomach (G–I), for the 11 study patients. Dose metrics of D1.0 cm^3, D3.0 cm^3, and D9.0 cm^3 are shown for each organ at risk. Each dose difference value is shown as a blue circle, with the thick black horizontal line indicating the mean dose difference value, and the vertical lines indicating the standard deviation for a given patient.

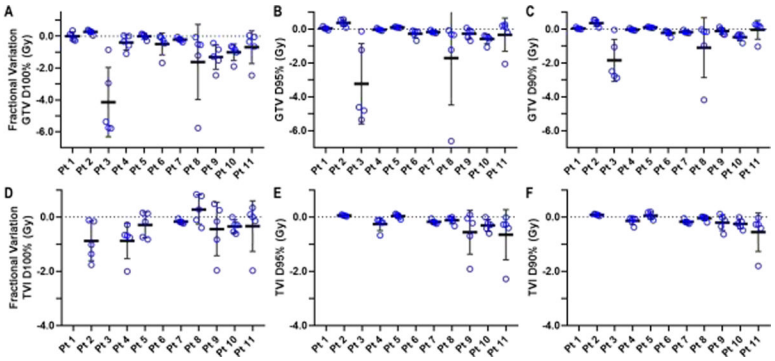

Fig. 4.

Variation in interfractional dose to the gross tumor volume (GTV), measured as the absolute dose difference between the plan metric value and that of each fractional accumulated value, for (A) D100%, (B) D95%, and (C) D90%, as well as interfractional dosimetric varaitions in tumor vessel interface (TVI) for (D) D100%, (E) D95%, and (F) D90% for the 11 study patients. Each dose difference value is shown as a blue circle, with the thick black horizontal line indicating the mean dose difference value, and the vertical line indicating the standard deviation for a given patient.

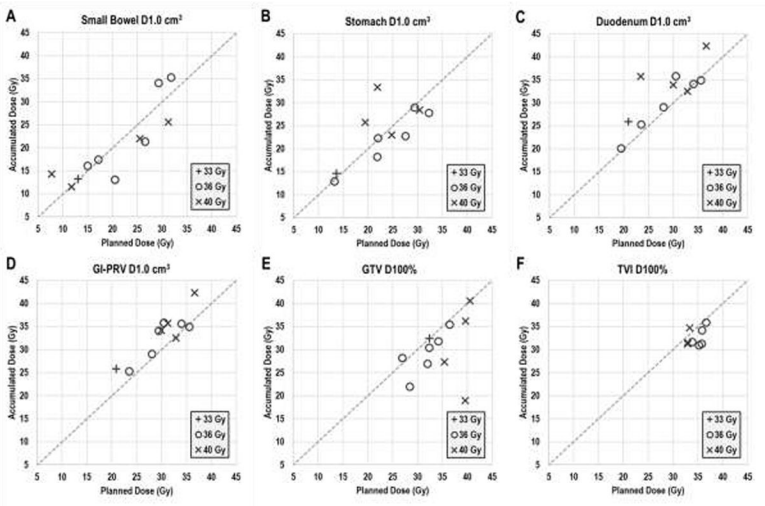

Fig 5.

Planned (x axes) vs. fiducial-aligned, accumulated (y axes) dose to 1.0 cm^3 of the (A) small bowel, (B) stomach, (C) duodenum, and (D) gastrointestinal planning organ-at-risk volume (GI-PRV), as well as the 100% coverage dose to the (E) gross tumor volume (GTV) and the (F) tumor vessel interface (TVI). All data points are grouped according to prescription dose. Large variances in D1.0 cm^3 were observed for all organs at risk, and several patients had notable reductions in GTV dose coverage, according to accumulated dose.

Table 1.

Dosimetric comparison of planned vs. accumulated doses to the gross tumor volume, tumor vessel interface, duodenum, small bowel, and stomach for 11 patients who underwent stereotactic body radiation therapy for pancreatic cancer. Absolute total dose difference is represented as the median value for the study population. The median fractional dose difference is the total average of the study population's median fractional dose difference between the planned value (scaled by dividing total dose by 5) and the fractional dose for each patient's 5 treatment fractions. Paired Wilcoxon signed-rank tests were used to compare accumulated vs. total planned dose metrics.

Structure and Dose Metric	Median Planned Dose, Gy (range)	Median Accumulated Dose, Gy (range)	Abs. Total Dose Difference, Gy (range)	Median Fractional Dose Difference, Gy (range)	*P* Value
Small Bowel					
D0.1 cm^3	24.55 (9.08–33.91)	18.16 (12.44–36.34)	−0.04 (−9.82–8.15)	0.20 (−1.15–1.90)	0.7002
D0.3 cm^3	22.84 (8.61–33.22)	17.92 (12.06–36.00)	0.11 (−8.73–7.49)	0.02 (−1.75–1.50)	0.6311
D1.0 cm^3	20.46 (7.75–31.85)	17.43 (11.47–35.24)	0.16 (−7.36–6.50)	0.03 (−1.47–1.30)	0.7647
D3.0 cm^3	17.83 (6.20–29.42)	16.53 (10.70–33.38)	−0.22 (−6.97–5.52)	−0.04 (−1.39–1.10)	0.7002
D9.0 cm^3	15.45 (3.48–25.41)	15.06 (8.51–29.61)	−0.32 (−7.44–6.75)	−0.07 (−1.49–1.35)	0.8311
Stomach					
D0.1 cm^3	25.37 (14.14–33.36)	26.55 (15.36–40.03)	0.68 (−3.98–16.38)	0.14 (−0.80–3.28)	0.8984
D0.3 cm^3	24.00 (13.80–33.01)	25.01 (14.28–37.35)	0.30 (−3.81–14.44)	0.10 (−0.76–3.01)	0.8984
D1.0 cm^3	22.02 (13.22–32.25)	22.97 (12.89–33.36)	−0.50 (−4.80– 11.43)	−0.10 (−0.96–2.29)	0.5772
D3.0 cm^3	20.77 (11.81–30.46)	21.48 (11.69–29.01)	−1.50 (−6.27–8.61)	−0.30 (−1.25–1.72)	0.4131
D9.0 cm^3	18.99 (9.65–27.04)	18.85 (10.34–24.93)	−1.36 (−9.03–6.90)	−0.27 (−1.81–1.38)	0.3203
Duodenum					
D0.1 cm^3	31.38 (20.81–39.16)	35.31 (22.21–43.88)	2.39 (−0.32–11.96)	0.48 (−0.06–2.39)	0.0068 *
D0.3 cm^3	31.01 (20.37–38.35)	34.84 (21.27–43.31)	1.89 (−0.42–12.47)	0.38 (−0.08–2.50)	0.0098 *
D1.0 cm^3	29.99 (19.45–36.64)	33.86 (20.04–42.29)	1.76 (−0.69–12.28)	0.35 (−0.14–2.46)	0.0137 *
D3.0 cm^3	28.54 (17.66–34.94)	31.35 (18.47–39.37)	1.70 (−1.27–110.69)	0.34 (−0.25–2.14)	0.0186 *
D9.0 cm^3	25.54 (12.25–32.74)	27.56 (15.10–33.34)	2.25 (−2.05–8.28)	0.45 (−0.41–1.66)	0.0186 *
GI-PRV					
D0.1 cm^3	31.82 (23.71–39.16)	35.91 (29.23–43.88)	4.51 (−0.32–8.34)	0.86 (−0.06–1.67)	0.0049 *
D0.3 cm^3	31.01 (22.72–38.35)	35.56 (27.51–43.34)	4.62 (−0.42–6.69)	0.92 (−0.08–1.34)	0.0049 *
D1.0 cm^3	30.44 (20.92–36.64)	34.18 (25.25–42.29)	4.19 (−0.69–5.66)	0.84 (−0.14–1.13)	0.0049 *
D3.0 cm^3	28.78 (17.80–34.94)	32.25 (21.93–39.37)	2.88 (−1.27–6.79)	0.58 (−0.25–1.36)	0.0098 *
D9.0 cm^3	25.61 (12.83–32.74)	27.92 (15.88–33.34)	2.83 (−2.05–5.31)	0.57 (−0.41–1.06)	0.0244 *
GTV					
Mean dose	36.98 (34.65–42.21)	36.41 (34.17–41.75)	−0.68 (−2.24–1.25)	0.03 (−0.45–0.25)	0.5195
D100%	34.23 (26.89–40.56)	30.36 (18.91–40.53)	−2.45 (−20.70–1.35)	−0.49 (−4.14–0.27)	0.0098 *
D98%	35.37 (28.76–40.80)	32.04 (23.17–41.31)	−1.71 (−17.30–1.78)	−0.34 (−3.46–0.36)	0.0322 *
D95%	35.76 (29.68–40.88)	33.05 (24.56–41.41)	−1.35 (−16.13–1.84)	−0.27 (−3.23–0.37)	0.0830

Structure and Dose Metric	Median Planned Dose, Gy (range)	Median Accumulated Dose, Gy (range)	Abs. Total Dose Difference, Gy (range)	Median Fractional Dose Difference, Gy (range)	*P* Value
D90%	36.13 (30.72–41.32)	34.39 (31.68–41.48)	−0.55 (−9.20–1.83)	−0.11 (−1.84–0.37)	0.1231
TVI					
Mean dose	38.65 (36.37–42.13)	38.33 (36.26–42.10)	−0.07 (−0.24–0.45)	−0.02 (−0.22–0.09)	0.2500
D100%	34.55 (32.93–36.69)	31.56 (30.87–35.84)	−1.70 (−4.41–1.39)	−0.34 (−0.88–0.28)	0.0234*
D98%	36.60 (33.88–40.55)	34.85 (32.49–38.99)	−1.70 (−3.35–0.01)	−0.34 (−0.67–0.01)	0.0391*
D95%	36.75 (34.17–41.20)	35.65 (33.29–40.61)	−1.09 (−3.26–0.28)	−0.22 (−0.65–0.06)	0.0391*
D90%	37.13 (34.79–41.36)	36.41 (34.49–41.14)	−0.22 (−2.78–0.41)	−0.16 (−0.56–0.08)	0.0781

Abbreviations: ABS, absolute; GI-PRV, gastrointestinal planning organ-at-risk volume; GTV, gross tumor volume; TVI, tumor vessel interface.

*$P<0.05$ indicates a significant difference.